THE JOURNAL OF BIOLOGICAL CHEMISTRY VOL. 286, NO. 42, pp. 36921–36931, October 21, 2011

Transcriptional Regulation of Neural Retina Leucine Zipper (*Nrl*), a Photoreceptor Cell Fate Determinant*

Received for publication, July 3, 2011, and in revised form, August 17, 2011 Published, JBC Papers in Press, August 24, 2011, DOI 10.1074/jbc.M111.279026

Cynthia L. Montana[‡], Karen A. Lawrence[‡], Natecia L. Williams[‡], Nicholas M. Tran[§], Guang-Hua Peng[§], Shiming Chen[§¶], and Joseph C. Corbo[‡‖1]

From the Departments of [‡]Pathology and Immunology, [§]Ophthalmology and Visual Sciences, [¶]Developmental Biology, and [‖]Genetics, Washington University School of Medicine, St. Louis, Missouri 63110

Background: The transcription factor *Nrl* is required for rod photoreceptor development, but mechanisms governing *Nrl* transcription remain largely unknown.
Results: The transcription factors CRX, OTX2, and RORβ regulate *Nrl* by binding directly to its promoter region.
Conclusion: These three factors combinatorially control *Nrl* expression in the developing mouse retina.
Significance: This study elucidates a critical link in the photoreceptor *cis*-regulatory network.

The transcription factor neural retina leucine zipper (*Nrl*) is a critical determinant of rod photoreceptor cell fate and a key regulator of rod differentiation. *Nrl*$^{-/-}$ rod precursors fail to turn on rod genes and instead differentiate as cones. Furthermore, *NRL* mutations in humans cause retinitis pigmentosa. Despite the developmental and clinical significance of this gene, little is known about the transcriptional regulation of *Nrl* itself. In this study, we sought to define the *cis*- and *trans*-acting factors responsible for initiation and maintenance of *Nrl* transcription in the mouse retina. Utilizing a quantitative mouse retinal explant electroporation assay, we discovered a phylogenetically conserved, 30-base pair region immediately upstream of the transcription start site that is required for *Nrl* promoter activity. This region contains binding sites for the retinal transcription factors CRX, OTX2, and RORβ, and point mutations in these sites completely abolish promoter activity in living retinas. Gel-shift experiments show that CRX, OTX2, and RORβ can bind to the critical region *in vitro*, whereas ChIP experiments demonstrate binding of CRX and OTX2 to the critical region *in vivo*. Thus, our results indicate that CRX, OTX2, and RORβ directly regulate *Nrl* transcription by binding to critical sites within the *Nrl* promoter. We propose a model in which *Nrl* expression is primarily initiated by OTX2 and RORβ and later maintained at high levels by CRX and RORβ.

NRL is a Maf family transcription factor that is required for mouse rod photoreceptor development (1). *Nrl* is expressed in the wild-type retina starting around embryonic day 12 (2), coincident with the beginning of the rod birth period (3, 4). It subsequently activates numerous rod-specific genes, including *Rhodopsin* (5, 6) and many components of the rod-specific phototransduction cascade (7, 8). NRL simultaneously represses cone genes in rods, either directly (9) or by activating the downstream repressor *Nr2e3* (10–13). In the *Nrl*$^{-/-}$ retina, rod gene expression fails to initiate, and rod precursors show a derepression of cone genes, which results in a transfating of the cells into cones in the adult retina (1, 14). *Nrl* expression is the earliest known marker of rod photoreceptor identity, and expression persists at high levels in the outer nuclear layer throughout adulthood. Not surprisingly, mutations in human *NRL* often result in heritable retinal disease, most commonly autosomal dominant retinitis pigmentosa.

Despite the importance of *Nrl* in the photoreceptor transcriptional network as well as in human disease, the mechanisms by which *Nrl* transcription is regulated are incompletely understood. Akimoto and colleagues (2) have shown that a 2.5-kb region upstream of *Nrl* is sufficient to drive GFP expression in rod photoreceptors. However, specific binding sites for transcriptional regulators within this promoter region remain unknown. An earlier study of the *Nrl* promoter (15) utilized a heterologous cell culture assay to identify promoter elements responsive to the rod fate inducer retinoic acid (16), but these sites have not yet been tested *in vivo*. *Nrl* has also been hypothesized to be a regulatory target of other retinal transcription factors such as CRX (17, 18) and RORβ (19), but it is unclear whether this regulation is direct or indirect. In this study, we sought to identify discrete *cis*-regulatory motifs and the transcription factors that bind them to regulate activation of the *Nrl* promoter.

To conduct the *Nrl* promoter analysis in the living mouse retina, we utilized a retinal explant electroporation assay (20). This assay has been used previously to quantify the activity of photoreceptor-specific *cis*-regulatory regions (21) and represents a much more realistic assay for analyzing *cis*-regulation than traditional mammalian cell culture approaches. Using this system, we have found that three retinal transcription factors, OTX2, CRX, and RORβ, activate *Nrl* transcription by binding directly to a highly conserved region of the *Nrl* promoter.

EXPERIMENTAL PROCEDURES

Mouse Husbandry—Adult CD1, C57BL/6, *Crx*$^{-/-}$ (22) and *Otx2*$^{f/f}$ (23) mice were maintained on a 12-h light/dark schedule

* This work was supported, in whole or in part, by National Institutes of Health, NEI Grant EY018826 (to J. C. C.) and Institutional Vision Science Training Grant 5-T32-EY13360-08 (to C. L. M. and N. M. T.). This work was also supported by The Hope Center for Neurologic Diseases (to J. C. C.) and The Children's Discovery Institute (to J. C. C.).
[1] To whom correspondence should be addressed: Dept. of Pathology and Immunology, Washington University School of Medicine, 660 S. Euclid Ave., Campus Box 8118, St. Louis, MO 63110. Fax: 314-362-7765; E-mail: jcorbo@pathology.wustl.edu.

TABLE 1
Sequences of sense primers used in site-directed mutagenesis reactions

Construct no.	Sequence of site-directed mutagenesis sense primer (mutated nucleotides underlined), 5′ to 3′
1	TTAACTTCTGGAGTTTCGGGGCGACACGCACCTATTTAAACAGC
2	GAGTTTCTTTTATCACATACAAGCGGGAAACAGCTTCAGGCAGG
3	TATCACAGCACCTATTTCCCACTAGGAAGGCAGGTTTAAACATC
4	CCTATTTAAACAGCTTCCTTACTTGGGAAACATCTCCTTGGCTA
5	CAGCTTCAGGCAGGTTTCCCACGAGAATTGGCTAAGTCCTACTA
6	CAGGTTTAAACATCTCCGGTTAGCCTGCCTACTATCCCTGCTTC
7	CATCTCCTTGGCTAAGTAAGCAGCGAACTGCTTCGGCCCCTACT
8	GCTAAGTCCTACTATCCAGTAGGGCCGCCCTACTAGGGGGTGAC
9	ACTATCCCTGCTTCGGCAAAGCAGCTTGGGTGACAGCTCTAAGA
10	CTTCGGCCCCTACTAGGTTTGTCACTATCTAAGAGGCGTTAGGC
11	TACTAGGGGGTGACAGCGAGCCTCTTAGTTAGGCGATTAGGCTG
12	TGACAGCTCTAAGAGGCTGGTCCGTCGTAGGCTGAAAATGTAGG
13	AAGAGGCGTTAGGCGATGCTTAGTCCCATGTAGGTCACACCCCA
14	AGGCGATTAGGCTGAAACGTGCTTGACCACCCCAGCCGTCTGGG
15	GCTGAAAATGTAGGTCAACAAAACTAAGTCTGGGAATGAGCGAG
16	TAGGTCACACCCCAGCCTGAGTTTCCGGAGCGAGAGAGGAGAAG

at 22 °C with free access to food and water. The *Otx2*$^{f/f}$ mutant (accession no. CDB0013K, Riken BioResource Center) was obtained as described (23). The health of the animals was regularly monitored. All studies were conducted in accordance with the Guide for the Care and Use of Laboratory Animals and the Animal Welfare Act and were approved by the Washington University in St. Louis Institutional Animal Care and Use Committee (approval no. 20110089).

DNA Constructs—The p*Nrl*(3.2 kb)-DsRed and pCAG-GFP vectors have been described previously (20, 24). p*Nrl*(3.2 kb)-GFP was created by replacing the DsRed coding sequence in p*Nrl*(3.2 kb)-DsRed with GFP, using the EcoRI and NotI restriction sites.

To create the *Nrl* promoter truncation constructs in Fig. 1, PCR was used to amplify the following regions of the mouse *Nrl* promoter relative to the transcription start site (RefSeq NM_001136074): p*Nrl*(2.9 kb), −2063 to +865; p*Nrl*(2.5 kb), −1695 to +865; p*Nrl*(1.1 kb), −202 to +865; p*Nrl*(0.8 kb), +35 to +865; and p*Nrl*(0.3 kb), +549 to +865. The promoter fragments were subcloned upstream of DsRed in the no-basal vector (17) using the XbaI and SmaI restriction sites.

Scanning mutagenesis constructs were created via site-directed mutagenesis of p*Nrl*(1.1 kb)-DsRed. The QuikChange II XL Site-Directed Mutagenesis kit (Agilent, Santa Clara, CA) was used with the primers listed in Table 1. (Both sense and antisense primers were added to the mutagenesis PCR reaction although only sense primers are listed.) In general, G↔T and C↔A substitutions were made unless mutagenesis generated a CRX binding site (constructs 8 and 12), in which case the *de novo* site was disrupted by an alternative substitution. Site-directed mutagenesis was also used to create one- or two-nucleotide mutations in the CRX and RORβ binding sites within the p*Nrl*(1.1 kb)-DsRed vector.

To create the CR-DsRed construct, the following oligonucleotides containing the *Nrl* critical region were kinased and annealed (restriction site-compatible ends underlined): 5′- ctagagttaggcgattaggctgaaaatgtaggtcacacccggtac-3′ and 5′-cgggtgtgacctacattttcagcctaatcgcctaact-3′, and the resultant product was subcloned upstream of DsRed in the *Rho*-basal vector (17) with the XbaI and KpnI restriction sites. To create (Rho-prox)-DsRed, a 205-nucleotide region of the mouse *Rho* promoter was obtained by PCR from mouse genomic DNA using the following primers: 5′-gtactctagaatgtcaccttggcccctc-3′ and 5′-gtacggtaccgacagagaccaaggctgct-3′. This product was digested with XbaI and KpnI and subcloned upstream of DsRed in the no-basal vector. (CR)-(Rho-prox)-DsRed and mutation-containing variants (see Fig. 2*C*) were created by subcloning CR[2]-containing oligonucleotides into the (Rho-prox)-DsRed vector with the restriction sites SalI and XbaI.

To create the *Nrl* promoter truncation constructs in Fig. 3, PCR was used to amplify the following regions of the mouse *Nrl* promoter relative to the transcription start site: p*Nrl*(0.99 kb), −122 to +865; p*Nrl*(0.97 kb), −102 to +865; p*Nrl*(0.95 kb), −82 to +865; and p*Nrl*(0.92 kb), −57 to +865. The promoter fragments were subcloned upstream of DsRed in the no-basal vector (17) using the XbaI and SmaI restriction sites.

Two non-fluorescent DNA constructs were electroporated in this study. The *Crx* RNAi construct has been described previously by Matsuda and Cepko (20). p*Nrl*(1.1 kb)-Cre was created by subcloning the Cre-coding sequence from pCAG-Cre (24) in place of DsRed in the p*Nrl*(1.1 kb)-DsRed vector, using the restriction sites EcoRI and NotI.

Electroporation and Culture of Explanted Retinas—Electroporation and explant culture of mouse retinas were performed as described previously (17). Briefly, eyes were removed from decapitated P0 mouse pups, and the retinas were dissected, leaving the lens in place. The retinas were then electroporated in a DNA solution consisting of the experimental DsRed reporter construct and a control GFP reporter construct, each at a final concentration of 0.5 μg/μl. Following the explant culture period, retinas were fixed, whole-mounted for quantitative imaging, and embedded for cryo-sectioning as described previously (21). Wild-type CD1 mice were used unless otherwise stated.

Quantitation of Promoter Activity in Whole-mount Retinas—DsRed fluorescence levels were measured and normalized to control GFP values as described previously (21). Briefly, eight to nine whole-mounted electroporated retinas for each reporter construct were imaged at 40× magnification under epifluorescent illumination. Images were captured in both the red and green channels using a monochromatic camera (ORCA-ER; Hamamatsu, Japan). Circles of interest were defined and mean pixel values were recorded for five regions overlying the electroporated retina and three control regions outside the retina (for background subtraction) in both the red and green channels using ImageJ software (National Institutes of Health, Bethesda, MD). For normalization, the background-subtracted mean pixel value of the experimental red channel was divided by the background-subtracted mean pixel value of the control green channel. S.D. was calculated based on all normalized fluorescence measurements (five measurements per retina, eight to nine retinas per construct).

Reverse Transcription Quantitative PCR for Nrl Transcript—Retinal tissue was isolated from wild-type (C57BL/6) and *Crx*$^{-/-}$ mice (on a C57BL/6 background). Three biological replicates (three to four retinas each) were collected for each time

[2] The abbreviations used are: CR, critical region; qPCR, quantitative real-time PCR; P12, postnatal day 12.

point. Total RNA was extracted using TRIzol (Invitrogen) and quantified using a Nanodrop device (Thermo Fisher Scientific). cDNA was synthesized using the Superscript III First-Strand Synthesis System for RT-PCR (Invitrogen) with 1 μg total RNA and oligo(dT)$_{20}$ primers. Reverse transcription quantitative PCR (RT-qPCR) was performed using SYBR-Green (Applied Biosystems, Carlsbad, CA) and the following primers (25): *Nrl* transcript, 5′-aacttctgagcatcgtggca-3′ and 5′-tgaagagtcgtgacctgcaaa-3′; GAPDH transcript, 5′-ctccactcacggcaaattca-3′ and 5′-cgctcctggaagatggtgat-3′. Three technical replicate PCRs were performed for each biological replicate. For each biological replicate, *Nrl* transcript levels were normalized to control GAPDH levels (ΔC_t). ΔC_t values from the three biological replicates were then averaged, and fold change relative to the wild-type P7 *Nrl* expression level was calculated, along with the S.D. across the biological replicates.

EMSA—The DNA binding domains of *Otx2* and *Rorb* were amplified from mouse retinal cDNA using the following PCR primers: *Otx2*, 5′-ttcgggaattccagcgaagggagaggacga-3′ and 5′-tcaggcggccgcctgctgttggcggcacttag-3′; *Rorb*, 5′-ttcgggaattcatgtgtgagaaccagcc-3′ and 5′-tcaggcggccgcagcctttgctgatgcttctg-3′. The products were digested with EcoRI and NotI and subcloned into the pGEX-5X-1 vector (Amersham Biosciences/GE Healthcare) to generate an N-terminal GST fusion. A third GST fusion vector containing the DNA binding domain of *Crx* has been described previously (21). The vectors were transformed into the *Escherichia coli* strain BL21, and recombinant protein was generated, purified, and concentrated as described previously (21).

Sense and antisense oligonucleotides were biotinylated with the biotin 3′ end DNA labeling kit (Pierce) per the manufacturer's instruction and annealed. For CRX and OTX2, DNA binding reactions were carried out at 25 °C for 1 h in the following 20-μl reaction mixture: 1 μl of recombinant protein, 1 fmol/μl biotinylated probe, 60 mM KCl, 25 mM HEPES (pH 7.6), 1 mM DTT, 1 mM EDTA, 5% glycerol. For RORβ, binding reactions were carried out at 25 °C for 1 h in the following 20-μl reaction mixture: 1× binding buffer (Pierce), 2.5% glycerol, 5 mM $MgCl_2$. Unlabeled, annealed competitor oligonucleotides were added to control reactions at a final concentration of 0.2 pmol/μl (200-fold molar excess relative to labeled probe). The binding reactions were run on a 10% Tris/borate/EDTA native polyacrylamide gel (Invitrogen) at 100 V for 30 min. Transfer to a nylon membrane, cross-linking of DNA to the membrane, blocking, incubation with streptavidin-horseradish peroxidase conjugate, washing, and chemiluminescent development were performed as directed by the LightShift Chemiluminescent EMSA Kit (Pierce).

ChIP—ChIP assays were performed as described previously (18) with minor modifications. Briefly, six to eight retinas were isolated from CD1 mice at each time point for each biological replicate (two biological replicates per time point, per antibody). Pooled retinas were cross-linked with 1% formaldehyde for 15 min at room temperature; the reaction was stopped by addition of glycine to a final concentration of 0.125 M. Cross-linked retinas were mechanically dissociated with a mortar and pestle and lysed in 0.5% Nonidet P-40. The nuclear pellet was lysed with 1% SDS and 0.5% EmpigenBB and homogenized by sonication, 35–50 × 10 s. at 25% amplitude (VibraCell; Sonics, Newtown, CT), to a chromatin fragment size range of 200–500 bp. Immunoprecipitation of sheared chromatin was performed overnight at 4 °C with 2.5 μg anti-CRX antibody (Santa Cruz Biotechnology, sc-30150X) or 2.5 μg anti-OTX2 antibody (Millipore, AB9566). Control precipitations were also carried out with 2.5 μg of rabbit IgG (Santa Cruz Biotechnology, sc-2027) for each biological replicate. Chromatin-antibody complexes were incubated with protein G Dynabeads (Invitrogen) for 2 h at 4 °C. After washing and elution steps, cross-links were reversed at 65 °C overnight. The immunoprecipitated DNA was purified using QIAquick purification columns (Qiagen, Valencia, CA).

qPCR was performed on immunoprecipitated, purified DNA using SYBR Green (Applied Biosystems) with the following primers: *Nrl* critical region, 5′-cctactaggggtgacagctc-3′ and 5′-tctcctctctcgctcattcc-3′; *Tyrobp* control, 5′-tctttctgcggccatgtcta-3′ and 5′-tgtgacgtccaaccaagtgaa-3′. Three technical replicate PCRs were performed for each of the two biological replicates. The fold enrichment of each target was calculated as 2 to the power of the cycle threshold (C_t) difference between IgG- and CRX-ChIP or IgG- and OTX2-ChIP.

RNA in Situ Hybridization—In situ hybridization on retinal tissue sections was performed as described previously (26). Briefly, either whole eyes or retinas were isolated from C57BL/6 mice at various time points. The tissue was fixed in 4% paraformaldehyde at 4 °C overnight, equilibrated in 30% sucrose/PBS, and embedded in OCT (Tissue Tek). The embedded tissue was cryosectioned, mounted on glass slides, and hybridized with RNA riboprobes synthesized from PCR products derived from templates described in previous studies (8, 17).

RESULTS

A 30-Nucleotide Region Is Critical for Nrl Promoter Activity—To identify the *cis*- and *trans*-acting factors required for regulation of *Nrl*, we undertook a detailed analysis of its proximal promoter region. A previous study demonstrated that a 3.2-kb fragment of the mouse *Nrl* promoter (from −2345 to +865 bp relative to the *Nrl* transcription start site) is sufficient to drive strong rod photoreceptor-specific expression in electroporated retinas (24). This fragment contains three blocks of high phylogenetic conservation (denoted P1, P2, and P3 in Fig. 1*A*), which correspond to regions bound by CRX *in vivo* as identified in a recent genome-wide ChIP-seq study (18). We created a series of *Nrl* promoter truncations to narrow down the minimal promoter region required for *Nrl* expression (Fig. 1*A*). These promoter truncations were fused to the fluorescent reporter DsRed and electroporated into P0 retinal explants along with the loading control p*Nrl*(3.2 kb)-GFP. The 3.2- and 2.9-kb constructs (both encompassing P1, P2, and P3) expressed strongly in explant cultures after 8 days (Fig. 1*B*). Interestingly, the 2.5- and 1.1-kb constructs that encompassed only P2 and P3 drove equally strong expression (Fig. 1*B*). Elimination of P2 in the 0.8- and 0.3-kb constructs, however, caused complete loss of p*Nrl*-DsRed expression, suggesting that P2 harbors *cis*-regulatory motifs critical for *Nrl* expression.

To identify these motifs within the P2 block, we performed scanning mutagenesis over a 160-bp region (Fig. 1*C*). Ten adja-

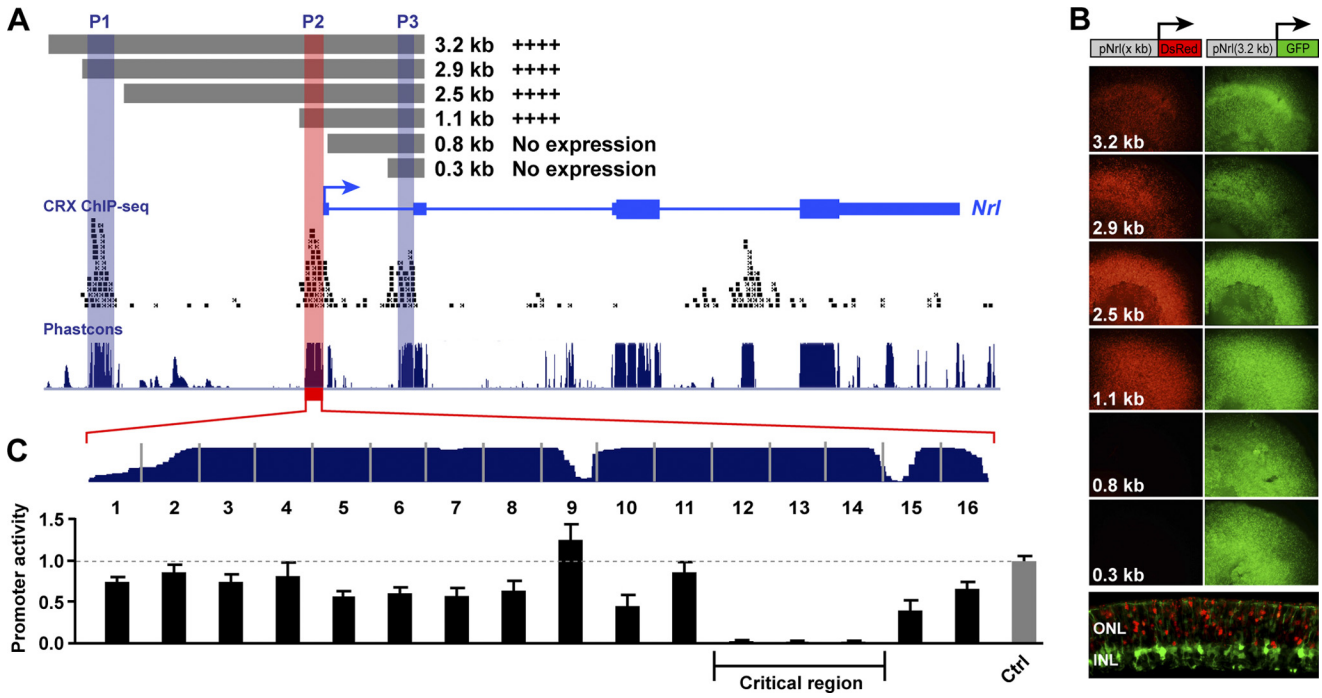

FIGURE 1. **Identification of a short, conserved region critical for *Nrl* promoter activity.** *A*, the fluorescent reporter DsRed was fused downstream of six different *Nrl* promoter truncations, ranging from 3.2 to 0.3 kb, based on blocks of phylogenetic conservation (P1, P2, and P3; University of California, Santa Cruz Genome Browser PhastCons track shown) (41) and previously published CRX ChIP-seq data (each *black tick mark* represents one sequence read) (18). *B*, p*Nrl*-DsRed truncation constructs were electroporated along with the p*Nrl*(3.2 kb)-GFP loading control into retinas dissected from P0 mice. After 8 days in explant culture the retinas were fixed and imaged in flatmount. Although the 3.2-, 2.9-, 2.5-, and 1.1-kb promoter truncations all drove similarly strong levels of DsRed expression, the 0.8- and 0.3-kb truncations failed to drive DsRed expression. DsRed expression was restricted to the outer nuclear layer for all constructs tested, as demonstrated in the cross-section of a retinal explant electroporated with p*Nrl*(3.2 kb)-DsRed and ubiquitously expressing pCAG-GFP (*bottom panel*). *C*, scanning mutagenesis was performed on a 160-bp region within the phylogenetically conserved block P2: using the p*Nrl*(1.1 kb)-dsRed construct as the vector backbone, 10 adjacent nucleotides of the P2 block were mutated at a time via site-directed mutagenesis (G↔T, A↔C). The 16 constructs were co-electroporated with p*Nrl*(3.2 kb)-GFP into P0 retinas, grown in explant culture for 8 days, and imaged in flatmount. p*Nrl*(1.1 kb, mutated)-DsRed expression, relative to pNrl(3.2 kb)-GFP expression, was quantified and normalized to wild-type pNrl(1.1 kb)-dsRed expression (*Ctrl*). Constructs 12, 13, and 14, encompassing 30 nucleotides total of the *Nrl* promoter, failed to drive DsRed expression. *Error bars* represent S.D.

cent nucleotides were mutated at a time via site-directed mutagenesis in the p*Nrl*(1.1 kb)-DsRed construct. The promoter activity of the 16 resultant constructs was then quantified by explant electroporation. Most mutations had relatively modest effects on promoter activity (Fig. 1*C*). However, constructs 12, 13, and 14, encompassing a 30-nucleotide block immediately upstream of the transcription start site, failed to drive any detectable DsRed expression. This 30-nucleotide span was denoted the "critical region" because of its indispensable role in *Nrl* promoter activity.

The Critical Region Contains Functional CRX- and RORβ-binding Sites—Examination of the 30-nucleotide critical region revealed near-consensus binding sites for two key photoreceptor transcription factors, CRX and RORβ, spaced seven nucleotides apart (Fig. 2*A*). The *Rorb* gene encodes two transcript isoforms, RORβ1 and RORβ2 (27), which encode proteins with somewhat different DNA-binding preferences. Whereas RORβ1 is widely expressed, RORβ2 is expressed preferentially in photoreceptors and the pineal gland (27). Interestingly, the AGGTCA core element of the putative RORβ site in the critical region of the Nrl promoter is immediately preceded by a thymidine nucleotide, which favors binding by the photoreceptor-enriched isoform RORβ2 (27).

To test the functionality of these two sites within the p*Nrl*(1.1 kb)-DsRed reporter, we created point mutations predicted to abolish CRX binding ("CRX mut") or RORβ binding ("RORβ mut1" and "RORβ mut2") (21, 27). All three constructs resulted in a complete loss of expression in retinal explants (Fig. 2*A*). Next, we tested whether the critical region has intrinsic promoter and/or enhancer activity (Fig. 2*B*). To test promoter activity, we cloned the critical region (CR) upstream of a minimal basal promoter from bovine rhodopsin which, by itself, does not drive any expression in photoreceptors (17). This construct failed to drive DsRed in explants (Fig. 2*B*, *top panels*). To determine whether the critical region could enhance the activity of an adjacent active promoter, we cloned it upstream of a promoter fragment from mouse rhodopsin ("Rho-prox"), which can drive moderate levels of DsRed expression by itself (Fig. 2*B*, *middle panels*). Fusion of the critical region to Rho-prox markedly boosted DsRed expression (Fig. 2*B*, *bottom panels*). Thus, the critical region lacks autonomous promoter activity but can act as a potent enhancer.

Lastly, we evaluated the relative contributions of the CRX and RORβ sites to the critical region enhancer activity (Fig. 2, *C* and *D*). Three new constructs were created on the (critical region)-(Rho-prox)-DsRed backbone, which eliminated the CRX site alone, the RORβ site alone, or both. These constructs were electroporated into retinal explants (Fig. 2*C*), and fluorescence levels were quantified (Fig. 2*D*). Mutation of the RORβ site elicited a greater reduction in enhancer activity than the CRX site mutation, whereas mutation of both sites caused an

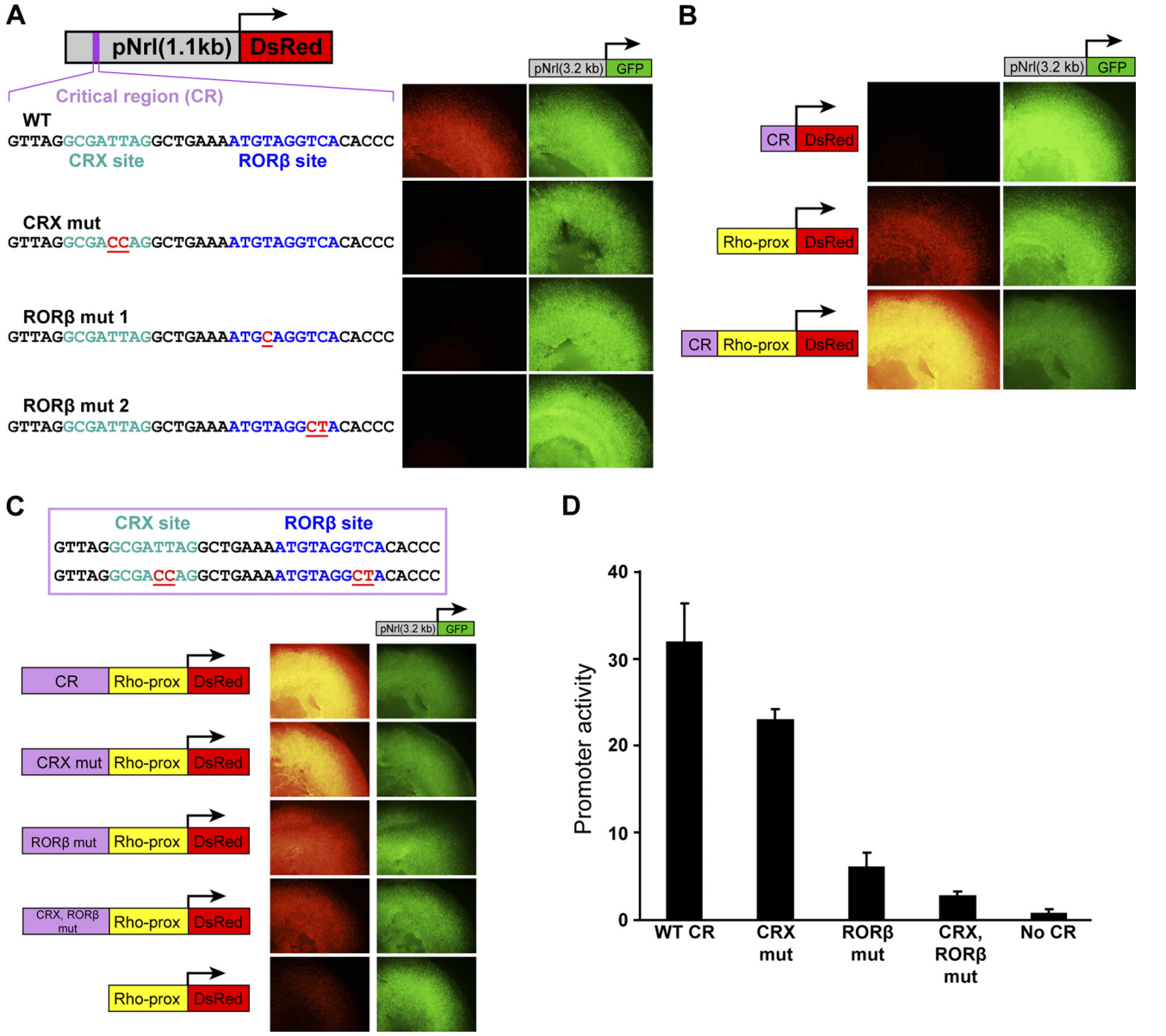

FIGURE 2. **Mutation of putative CRX and RORβ binding sites abolish the activity of the *Nrl* promoter critical region.** *A*, the critical region contains bioinformatically predicted binding sites for both CRX and RORβ. pNrl(1.1 kb)-DsRed constructs were created that contain point mutations predicted to abolish CRX binding (*CRX mut*) or RORβ binding (RORβ mut1 and RORβ mut2). All three mutant constructs failed to express in retinal explants. *B*, the critical region was isolated and fused to a basal promoter (123 nucleotides from the bovine rhodopsin promoter) and DsRed but failed to drive DsRed expression (*top panel*). The critical region was also fused to the short promoter Rho-prox (205 nucleotides from the mouse rhodopsin promoter). Although Rho-prox can autonomously drive moderate DsRed expression (*middle panel*), fusion of the critical region with Rho-prox greatly boosts DsRed expression (*bottom panel*). *C*, point mutations predicted to abolish binding of CRX, RORβ, or CRX and RORβ caused graded loss of promoter activity of the (critical region)-(Rho-prox)-DsRed construct. *D*, quantification of DsRed fluorescence of the constructs shown in *C*, normalized to (Rho-prox)-DsRed (*No CR*). *Error bars* represent S.D.

almost complete loss of critical region enhancer activity (Fig. 2*D*).

A Conserved Sequence Upstream of Critical Region Contains Additional cis-Motifs—With one exception, scanning mutagenesis of individual 10-bp blocks upstream of the critical region (constructs 1–11) resulted in modest decrements in promoter activity, in some cases down to ~50% of wild-type levels (Fig. 1*C*). This observation, and the fact that this region is highly conserved phylogenetically, suggested that it might contain multiple transcription factor binding sites that coordinately regulate promoter activity. To test this idea, we engineered five additional truncations of the *Nrl* promoter across this region and electroporated them into retinal explants as DsRed fusion constructs (Fig. 3, *A* and *B*). As quantified in Fig. 3*C*, graded truncation of the *Nrl* promoter correlated with graded loss of promoter activity (Fig. 3*C*). Thus, the 110-bp sequence immediately upstream of the *Nrl* critical region is indispensable for *Nrl* promoter activity, despite the fact that no specific 10-bp block within the region is strictly required for expression.

Coordinate Regulation of Nrl by CRX and OTX2—Explant electroporation experiments determined that a putative CRX-binding site is essential for *Nrl* promoter activity. In addition, a prior study showed a marked decrement in *Nrl* transcript levels in P28 $Crx^{-/-}$ retinas by *in situ* hybridization (17). To deter-

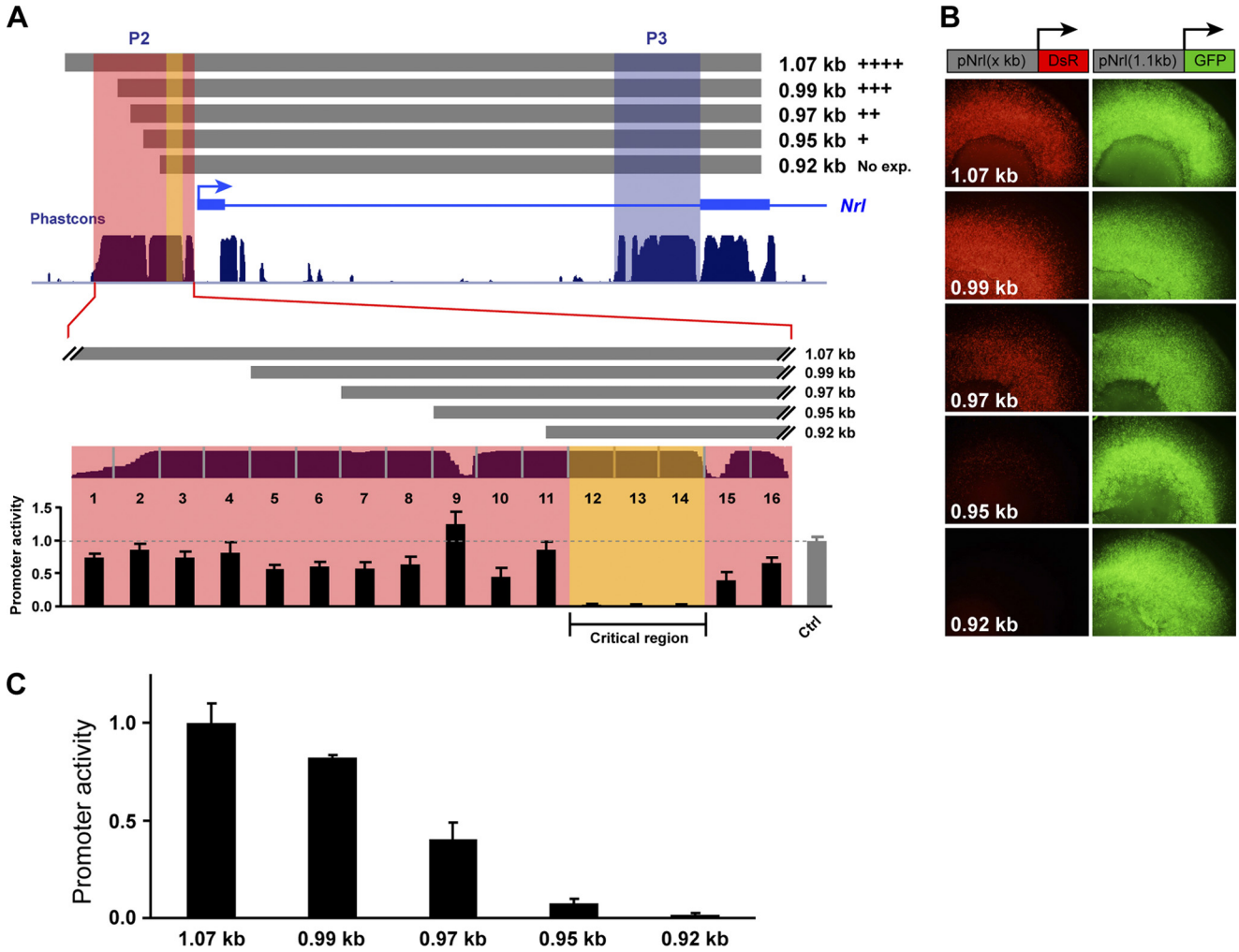

FIGURE 3. **Graded truncation of the *Nrl* promoter upstream of the critical region correlates with graded loss of promoter activity.** *A*, four additional *Nrl* promoter truncations, 0.99, 0.97, 0.95, and 0.92 kb, were fused to DsRed and electroporated into retinal explants. Note that the 1.07-kb promoter was referred to as 1.1 kb in Figs. 1 and 2. *B*, progressive truncation of the promoter region immediately upstream of the critical region correlated with graded loss of promoter activity. *C*, quantification of DsRed fluorescence of the constructs shown in *A* and *B*, normalized to p*Nrl*(1.07 kb)-DsRed. *Error bars* represent S.D.

mine the temporal dependence of *Nrl* expression on CRX, we measured *Nrl* transcript levels across developmental time in wild-type and $Crx^{-/-}$ retinas (Fig. 4*A*). RT-qPCR showed that *Nrl* transcript levels are similar in wild-type and $Crx^{-/-}$ retinas until P7, after which the levels fall off sharply in $Crx^{-/-}$ compared with wild-type (Fig. 4*A*). This result suggests that CRX is not required for the initiation of *Nrl* expression *in vivo* but that it is necessary for maintenance of *Nrl* transcription at later time points. In a second experiment, we co-electroporated p*Nrl*(3.2 kb)-DsRed and control pCAG-GFP into P0 wild-type and $Crx^{-/-}$ retinal explants. After 10 days in culture, p*Nrl*(3.2 kb)-DsRed expression was moderately reduced in $Crx^{-/-}$ explants relative to wild-type (Fig. 4*B*), confirming that CRX plays only a minor role in activating the *Nrl* promoter in the early postnatal period.

These two results are seemingly at odds with the observation that mutation of a single putative CRX-binding site within the critical region completely abolishes *Nrl* promoter activity in electroporated retinas in the early postnatal period (Fig. 2*A*). To account for this discrepancy, we hypothesized that the retinal transcription factor OTX2 might be able to compensate for CRX at early time points. OTX2 and CRX are both K50 homeodomain transcription factors required for photoreceptor development (28–30), and they have nearly identical DNA-binding preferences (21, 31). In addition, *Otx2* is required for initiation of *Crx* expression (30). *Otx2* and *Crx* are both expressed at high levels in differentiating photoreceptors through P3.5 (Fig. 4*C*). By P10.5, however, *Otx2* levels have decreased in photoreceptors, whereas *Crx* levels remain high (Fig. 4*C*). At the adult stage, expression of *Otx2* persists in photoreceptors at only very low levels, whereas *Crx* is maintained at high levels (17). Thus, it is reasonable to surmise that both OTX2 and CRX may bind to the *Nrl* promoter critical region in the early postnatal period to activate *Nrl* transcription. As photoreceptor OTX2 levels decline later, CRX may become the predominant activator of *Nrl*.

To test the hypothesis that both CRX and OTX2 activate the *Nrl* promoter in the early postnatal period, we performed a series of explant electroporations utilizing retinas from the $Otx2^{f/f}$ mouse, which is homozygous for a conditional ("floxed") allele of *Otx2* (Fig. 4*D*). Electroporation of p*Nrl*(3.2 kb)-DsRed and control pCAG-GFP into $Otx2^{f/f}$ explants resulted in strong DsRed expression after 10 days (Fig. 4*D*, *upper first panel*). To

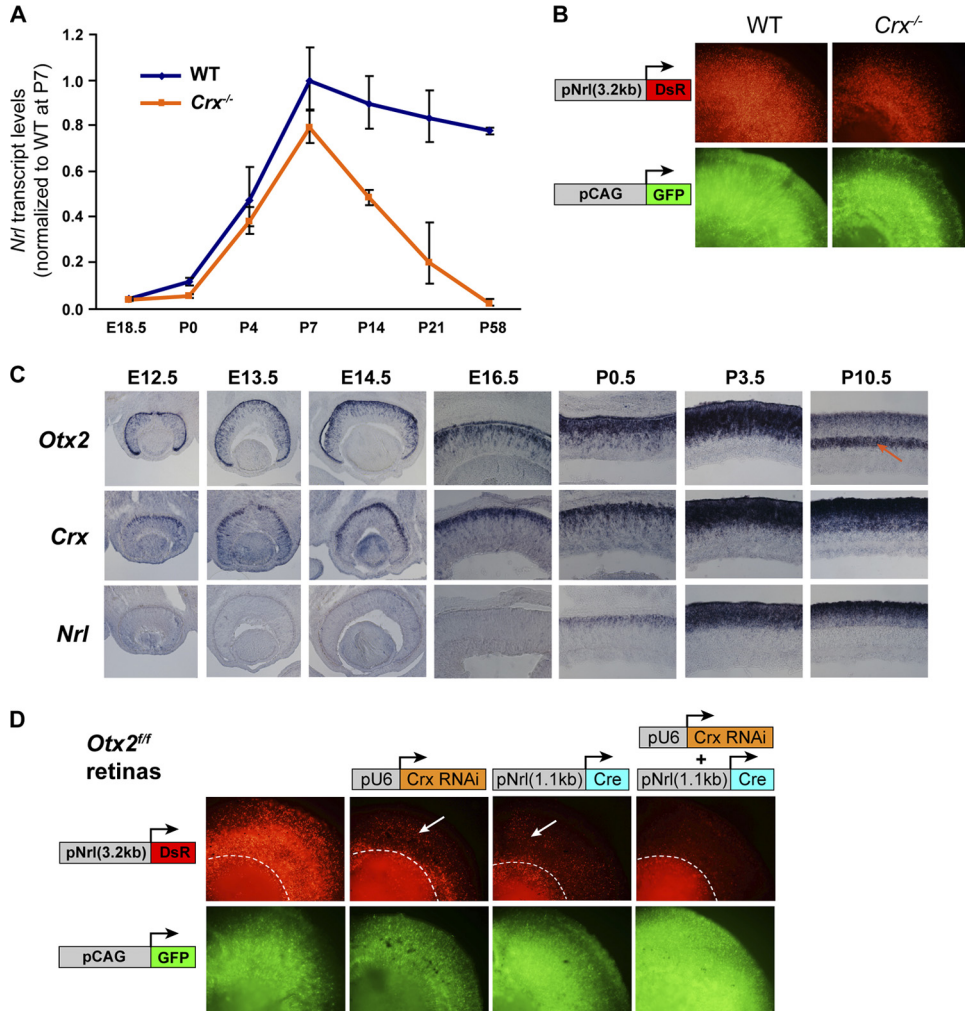

FIGURE 4. **CRX and OTX2 coordinately regulate *Nrl* expression in the developing mouse retina.** *A*, RT-qPCR analysis of *Nrl* transcript levels in C57BL/6 wild-type mice (*blue line*) and *Crx* null mice (*orange line*). *Error bars* represent S.D. across three biological replicates. *B*, wild-type and *Crx* null retinas were co-electroporated with p*Nrl*(3.2 kb)-DsRed and the pCAG-GFP loading control and cultured for 10 days. DsRed expression was modestly reduced in $Crx^{-/-}$ retinas compared with wild-type. *C*, *in situ* hybridizations for the *Otx2*, *Crx*, and *Nrl* transcripts in wild-type retinas at various developmental time points. The embryonic day 14.5, P3.5, and P10.5 *Crx* images have been previously published (17) and are reproduced here for the sake of comparison. Note that *Crx* and *Otx2* possess nearly identical expression patterns in the retina from embryonic day 12.5 through P3.5, with the exception that *Otx2* is also expressed in the retinal pigmented epithelium. However, after P3.5, *Otx2* levels diminish in the outer nuclear layer, whereas high *Crx* levels are sustained. The *orange arrow* at P10.5 denotes persistent, high level *Otx2* expression in bipolar cells of the inner retina. *D*, retinas from homozygous *Otx2* floxed mice ($Otx2^{f/f}$) were co-electroporated with p*Nrl*(3.2 kb)-DsRed and the pCAG-GFP and cultured for 10 days. Retinas that were additionally electroporated with CRX RNAi (*upper second panel*) or a Cre recombinase-encoding plasmid (*upper third panel*) showed a reduction in p*Nrl*(3.2 kb)-DsRed expression. Retinas that received both CRX RNAi and Cre recombinase (*upper fourth panel*) showed nearly undetectable levels of p*Nrl*(3.2 kb)-DsRed. Note that the fluorescence enclosed by the *white dashed lines* indicates lens autofluorescence. Residual DsRed expression in photoreceptors is indicated by *white arrows*.

eliminate CRX alone, we co-electroporated a CRX RNAi construct (20) along with the fluorescent reporters, which resulted in a decrease in p*Nrl*-DsRed expression (Fig. 4*D*, *upper second panel*). Interestingly, the decrease in expression was greater than what was observed when the p*Nrl*-DsRed construct was electroporated into $Crx^{-/-}$ retinas (Fig. 4*B*). This difference might be explained by the fact that in the $Crx^{-/-}$ retina, there is an ~2-fold increase in *Otx2* expression (17). Thus, in the acute RNAi-mediated knockdown of *Crx*, there may be insufficient time for compensatory *Otx2* up-regulation.

To acutely knock-out *Otx2* alone, we co-electroporated a plasmid encoding Cre recombinase along with the fluorescent reporters and again observed decreased p*Nrl*-DsRed expression (Fig. 4*D*, *upper third panel*). Because initiation of *Crx* expression depends on *Otx2* (30), one might expect that knock-out of *Otx2* would result in loss of both *Otx2* and *Crx*. However, some residual expression of the DsRed reporter was still apparent in photoreceptors when *Otx2* was knocked out (Fig. 4*D*, *upper third panel*). We therefore hypothesized that there may be some perdurance of *Crx* transcripts in *Otx2* knock-out. Thus, to decrease *Crx* and *Otx2* transcript levels simultaneously, we co-electroporated both CRX RNAi and Cre recombinase. This dual knockdown approach reduced p*Nrl*-DsRed expression to nearly undetectable levels (Fig. 4*D*, *upper fourth panel*), supporting our hypothesis that CRX and OTX2 are both necessary for activation of the *Nrl* promoter during rod photoreceptor development. In addition, these findings are consistent with the idea that both CRX and OTX2 mediate *Nrl* activation by binding to the "CRX" site present in the critical region.

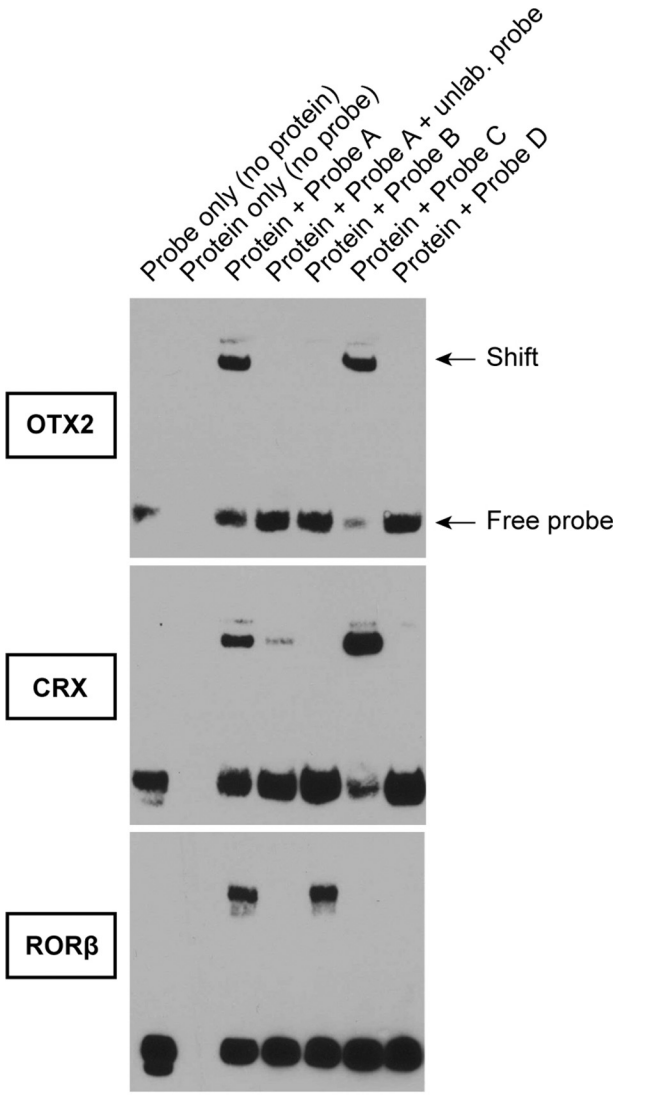

FIGURE 5. **EMSA shows that OTX2, CRX, and RORβ are capable of binding to the critical region *in vitro*.** Recombinant GST fusion proteins containing the DNA-binding domains of OTX2 (*top panel*), CRX (*middle panel*), and RORβ (*bottom panel*) were mixed with 35-bp biotinylated probes containing the *Nrl* promoter critical region (indicated at the *bottom*). All three proteins caused a shift of the probe containing the wild-type sequence (*Probe A*), and this shift was eliminated by the addition of unlabeled competitor probe (200-fold molar excess). A probe containing mutations in the CRX site (*Probe B*) was shifted by RORβ protein but not by OTX2 or CRX protein. A probe containing mutations in the RORβ site (*Probe C*) was shifted by OTX2 and CRX protein but not by RORβ protein. A probe containing mutations in both the CRX and RORβ sites was not shifted by any of the three proteins.

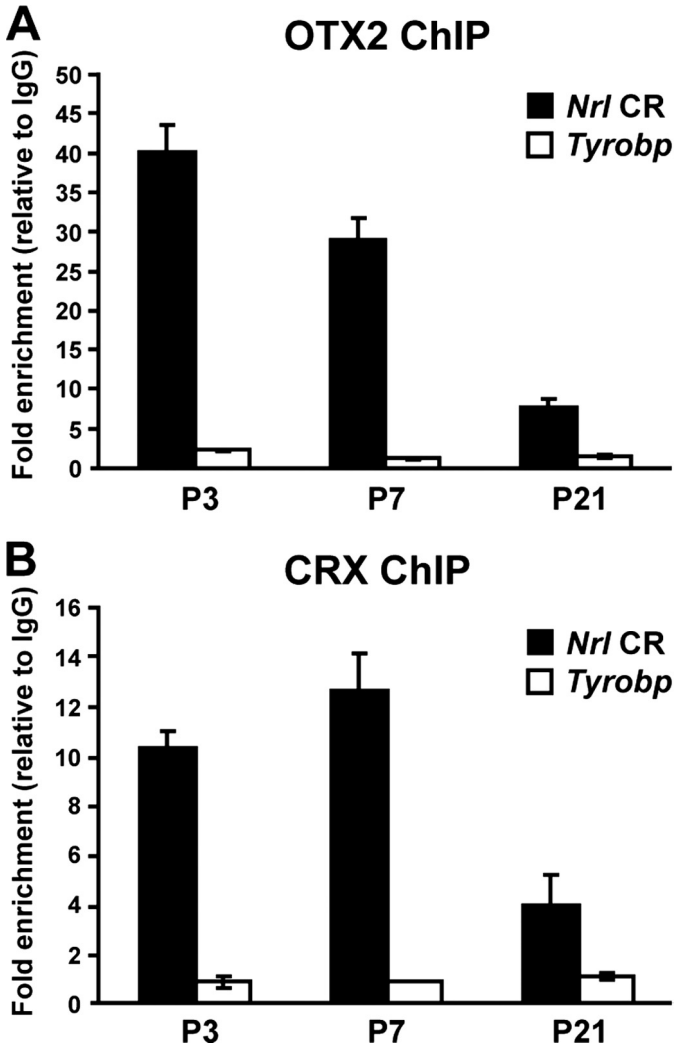

FIGURE 6. **ChIP demonstrates binding of OTX2 and CRX to the critical region *in vivo*.** ChIP was performed on retinal tissue isolated at P3, P7, and P21 utilizing antibodies to OTX2 (*top panel*) and CRX (*bottom panel*). Quantitative real-time PCR was performed to measure enrichment at the *Nrl* critical region (*Nrl CR*) and a negative control region not predicted to bind OTX2 or CRX (*Tyrobp*). *Error bars* represent S.D. between two biological replicates.

OTX2, CRX, and RORβ Bind Directly to Nrl Promoter—Next, we wished to determine whether OTX2, CRX, and RORβ bind the bioinformatically identified sites within the critical region of the *Nrl* promoter. First, we performed an EMSA with biotinylated probes containing the sequence of the critical region (Fig. 5). Recombinant proteins consisting of the DNA-binding domains of OTX2, CRX, and RORβ were purified, mixed with the probes, and run on a non-denaturing gel. OTX2 and CRX protein were both able to shift the biotinylated probe containing the wild-type critical region sequence (Fig. 5, *top two panels*, *third row*), and the shift was eliminated by non-biotinylated competitor probe (*fourth row*). Mutation of the CRX site alone completely abolished the shift (*fifth row*); mutation of the RORβ site alone did not affect the shift (*sixth row*); and mutation of both the CRX and RORβ sites again abolished the shift (*seventh row*). Likewise, RORβ was able to shift the wild-type probe (*bottom panel, third row*) and the probe containing a CRX mutation (*fifth row*) but was unable to shift the probes containing mutations of the RORβ site (*sixth row*) or RORβ and

CRX sites (*seventh row*). This result indicates that OTX2, CRX, and RORβ bind strongly and specifically to their cognate sites in the *Nrl* critical region *in vitro*.

To test whether OTX2, CRX, and RORβ bind to the *Nrl* critical region *in vivo*, we performed a chromatin immunoprecipitation experiment utilizing mouse retinal tissue isolated at three postnatal time points. Antibodies to OTX2 and CRX produced enrichment of the *Nrl* critical region at all three time points, with peak OTX2 binding at P3 and peak CRX binding at P7 (Fig. 6). As a control, the promoter of the microglial gene *Tyrobp*, which is not predicted to bind either CRX or OTX2, was not enriched. Two different polyclonal antibodies against RORβ did not show enrichment of the critical region (data not shown). However, these antibodies also failed to show enrichment of the blue cone opsin promoter region, which has been shown previously to be a direct target of RORβ (32). Thus, the absence of enrichment at the *Nrl* promoter in this case is likely attributable to the inability of these antibodies to immunoprecipitate their target.

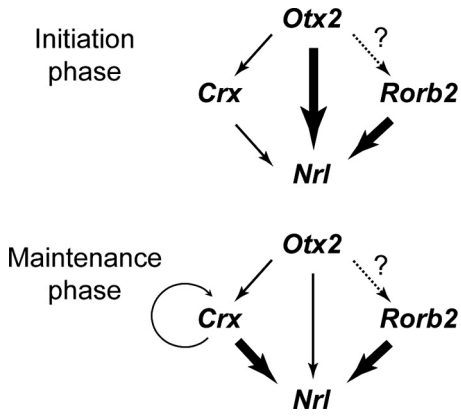

FIGURE 7. **Model for coordinate regulation of *Nrl* by transcription factors OTX2, CRX, and RORβ.** OTX2, CRX, and RORβ are hypothesized to contribute to *Nrl* expression in the early "initiation" phase, with OTX2 and RORβ playing a particularly important role (as indicated by *boldface arrows*). During the later "maintenance" phase of *Nrl* expression, CRX becomes a more important activator of *Nrl* as OTX2 levels decline in photoreceptors. Prior studies have suggested that CRX transcriptionally autoregulates.

DISCUSSION

In this study, we have shown that OTX2, CRX, and RORβ directly regulate *Nrl* expression in developing mouse rod photoreceptors. Binding sites for these factors reside in a highly conserved region immediately upstream of the *Nrl* transcription start site, and directed point mutations in these sites are sufficient to completely abolish p*Nrl*-DsRed expression in mouse retinal explants. EMSA experiments confirm direct binding of OTX2, CRX, and RORβ at this region of the *Nrl* promoter. Direct binding of OTX2 and CRX was further validated in ChIP experiments with mouse retinal lysates. While we were preparing our manuscript, a report appeared, which corroborates our findings with respect to the regulation of the *Nrl* promoter by RORβ (33).

An interesting conclusion from our experiments was the functional redundancy of CRX and OTX2 in the activation of *Nrl* transcription during the late embryonic and early postnatal periods. Both OTX2 and CRX are required for photoreceptor development (22, 28, 30) but because OTX2 is required for initiation of *Crx* transcription (30), it is difficult to distinguish the roles of these two transcription factors in the regulation of specific genes. A study utilizing the $Otx2^{+/CKO};Crx^{-/-}$ double knock-out suggested that OTX2 itself is an active regulator of certain photoreceptor genes in the early postnatal period, such as *Rho* and *Pde6b* (34). In the present study, we demonstrated by ChIP that OTX2 and CRX are both bound at the *Nrl* promoter at P3, P7, and P21. Moreover, OTX2 activation of *Nrl* can partially compensate for the loss of *Crx* in the first postnatal week, whereas loss of both OTX2 and CRX results in a dramatic loss of *Nrl* promoter activation. Our findings suggest the following model for the initiation and maintenance of *Nrl* transcription (Fig. 7). During the initiation phase, OTX2 and RORβ are the main activators of the *Nrl* promoter. In the later maintenance phase, however, CRX supplants OTX2 as the main activator of *Nrl* transcription.

Although our analysis has identified two critical *cis*-regulatory motifs in the *Nrl* promoter, there are undoubtedly a number of other important regulatory sites that remain unknown. For example, the 110-base pair region upstream of the critical region likely contains binding sites for multiple transcription factors that may act synergistically to activate *Nrl* expression. We found that disruption of individual sites via scanning mutagenesis is not sufficient to abolish *Nrl* promoter activity, whereas elimination of the entire 110-bp region causes total loss of activity. A couple of low affinity CRX sites are present in this region and may play a role in activation (data not shown). It is possible that binding sites for other factors are also present.

Retinoic acid has long been known to foster rod photoreceptor differentiation (16, 35); thus, retinoic acid receptors represent attractive candidate regulators of *Nrl* expression. Several years ago, Khanna and colleagues (15) identified three elements within the *Nrl* promoter region that appear to be sensitive to retinoic acid in a heterologous tissue culture assay system. We sought to test the importance of these putative retinoic acid response elements in living mouse retinas by mutating each retinoic acid response element individually in the context of the p*Nrl*(1.1 kb)-DsRed reporter. Mutation of the individual retinoic acid response elements resulted in only modest changes in DsRed expression relative to the non-mutated control (data not shown). Therefore, although these sites might contribute to the modulation of *Nrl* expression *in vivo*, they are not individually required for activation of the *Nrl* promoter.

A recent CRX ChIP-seq study found that many photoreceptor genes are surrounded by a spatially distributed network of CRX-bound regions that are hypothesized to act in a combinatorial fashion to regulate expression of their associated gene (18). The *Nrl* gene also appears to follow this pattern as a total of four highly conserved noncoding regions, which correspond to CRX ChIP-seq peaks, were identified around the locus: P1, P2, P3, and an element within the third intron (Fig. 1*A*). The initial promoter truncation analysis demonstrates that the P1 element is not critical for *Nrl* promoter activation, but P1 may be involved in fine-tuning of *Nrl* expression levels in rods. In addition, the P1 element may also contribute to maintenance of normal levels of *Nrl* expression at later developmental timepoints and in the adult.

The roles of the P3 region and the intronic element also remain to be explored. Preliminary bioinformatic analyses identified a potential CRX site in the P3 region, but point mutation of this site in the context of the full-length p*Nrl*(3.2 kb)-DsRed resulted in only minimal changes in expression (data not shown). It is possible that this region and the intronic element play a role in modulating *Nrl* expression outside the time window assayed in the present study.

The close proximity of the OTX2/CRX and RORβ binding sites in the *Nrl* promoter critical region is noteworthy. We previously showed that clusters and pairs of transcription factor binding sites, often within 50 bp of one another, are present in many photoreceptor *cis*-regulatory regions (17, 18). In fact, as few as three closely clustered CRX sites in the context of a synthetic *cis*-regulatory element are sufficient to drive photoreceptor-specific expression in electroporated retinas (18). Many endogenous photoreceptor *cis*-regulatory regions, however, appear to be comprised of clusters of both CRX sites and other sites for factors such as NRL, NR2E3, and bHLH factors such as NEUROD1 (9, 18, 36). Thus, the paired OTX2/CRX-RORβ motif identified in the present study obeys the usual logic of photoreceptor *cis*-regulatory grammar.

In conclusion, we have identified three transcription factors, OTX2, CRX, and RORβ, that control *Nrl* expression by direct binding to the *Nrl* promoter. Although all three of these factors are present in both rods and cones and are required for gene expression in both cell types (17, 19, 28–30, 32, 34), antibody and misexpression studies indicate that NRL is likely restricted to rods (37, 38). How then is the rod-specific pattern of *Nrl* expression established? One possibility is that a yet-undiscovered rod-specific transcription factor functions upstream of *Nrl* and coordinates with OTX2, CRX, and/or RORβ to activate *Nrl* transcription exclusively in rods. Alternatively, it is possible that there exists a cone-specific transcription factor X, which acts as a repressor of *Nrl* and thereby restricts its expression to rods. If NRL were to reciprocally repress factor X expression in rods, then the two factors could act together as a poised binary switch between rod and cone cell fate similar to what has been observed in a number of systems (39). Whereas knock-out of *Nrl* results in a transfating of rods into UV-sensitive cones (1), knock-out of factor X would be predicted to result in the converse phenotype. A recent study in zebrafish has identified such a factor: loss of *Tbx2b* results in a "lots of rods" phenotype in which UV cones are converted into rods (40). It will be extremely interesting to determine whether an analogous factor exists in mammalian retinas.

Acknowledgments—We thank the members of the Corbo lab for input and support during the course of this work. In addition, we thank Shinichi Aizawa for the Otx2$^{f/f}$ mice.

REFERENCES

1. Mears, A. J., Kondo, M., Swain, P. K., Takada, Y., Bush, R. A., Saunders, T. L., Sieving, P. A., and Swaroop, A. (2001) *Nat. Genet.* **29,** 447–452
2. Akimoto, M., Cheng, H., Zhu, D., Brzezinski, J. A., Khanna, R., Filippova, E., Oh, E. C., Jing, Y., Linares, J. L., Brooks, M., Zareparsi, S., Mears, A. J., Hero, A., Glaser, T., and Swaroop, A. (2006) *Proc. Natl. Acad. Sci. U.S.A.* **103,** 3890–3895
3. Young, R. W. (1985) *Anat. Rec.* **212,** 199–205
4. Cepko, C. L., Austin, C. P., Yang, X., Alexiades, M., and Ezzeddine, D. (1996) *Proc. Natl. Acad. Sci. U.S.A.* **93,** 589–595
5. Rehemtulla, A., Warwar, R., Kumar, R., Ji, X., Zack, D. J., and Swaroop, A. (1996) *Proc. Natl. Acad. Sci. U.S.A.* **93,** 191–195
6. Kumar, R., Chen, S., Scheurer, D., Wang, Q. L., Duh, E., Sung, C. H., Rehemtulla, A., Swaroop, A., Adler, R., and Zack, D. J. (1996) *J. Biol. Chem.* **271,** 29612–29618
7. Yoshida, S., Mears, A. J., Friedman, J. S., Carter, T., He, S., Oh, E., Jing, Y., Farjo, R., Fleury, G., Barlow, C., Hero, A. O., and Swaroop, A. (2004) *Hum. Mol. Genet.* **13,** 1487–1503
8. Corbo, J. C., Myers, C. A., Lawrence, K. A., Jadhav, A. P., and Cepko, C. L. (2007) *Proc. Natl. Acad. Sci. U.S.A.* **104,** 12069–12074
9. Peng, G. H., and Chen, S. (2005) *Vis. Neurosci.* **22,** 575–586
10. Oh, E. C., Cheng, H., Hao, H., Jia, L., Khan, N. W., and Swaroop, A. (2008) *Brain Res.* **1236,** 16–29
11. Corbo, J. C., and Cepko, C. L. (2005) *PLoS Genet.* **1,** e11
12. Chen, J., Rattner, A., and Nathans, J. (2005) *J. Neurosci.* **25,** 118–129
13. Peng, G. H., Ahmad, O., Ahmad, F., Liu, J., and Chen, S. (2005) *Hum. Mol. Genet.* **14,** 747–764
14. Daniele, L. L., Lillo, C., Lyubarsky, A. L., Nikonov, S. S., Philp, N., Mears, A. J., Swaroop, A., Williams, D. S., and Pugh, E. N., Jr. (2005) *Invest. Ophthalmol. Vis. Sci.* **46,** 2156–2167
15. Khanna, H., Akimoto, M., Siffroi-Fernandez, S., Friedman, J. S., Hicks, D., and Swaroop, A. (2006) *J. Biol. Chem.* **281,** 27327–27334
16. Kelley, M. W., Turner, J. K., and Reh, T. A. (1994) *Development* **120,** 2091–2102
17. Hsiau, T. H., Diaconu, C., Myers, C. A., Lee, J., Cepko, C. L., and Corbo, J. C. (2007) *PLoS ONE* **2,** e643
18. Corbo, J. C., Lawrence, K. A., Karlstetter, M., Myers, C. A., Abdelaziz, M., Dirkes, W., Weigelt, K., Seifert, M., Benes, V., Fritsche, L. G., Weber, B. H., and Langmann, T. (2010) *Genome Res.* **20,** 1512–1525
19. Jia, L., Oh, E. C., Ng, L., Srinivas, M., Brooks, M., Swaroop, A., and Forrest, D. (2009) *Proc. Natl. Acad. Sci. U.S.A.* **106,** 17534–17539
20. Matsuda, T., and Cepko, C. L. (2004) *Proc. Natl. Acad. Sci. U.S.A.* **101,** 16–22
21. Lee, J., Myers, C. A., Williams, N., Abdelaziz, M., and Corbo, J. C. (2010) *Gene Ther.* **17,** 1390–1399
22. Furukawa, T., Morrow, E. M., Li, T., Davis, F. C., and Cepko, C. L. (1999) *Nat. Genet.* **23,** 466–470
23. Tian, E., Kimura, C., Takeda, N., Aizawa, S., and Matsuo, I. (2002) *Dev. Biol.* **242,** 204–223
24. Matsuda, T., and Cepko, C. L. (2007) *Proc. Natl. Acad. Sci. U.S.A.* **104,** 1027–1032
25. Cicero, S. A., Johnson, D., Reyntjens, S., Frase, S., Connell, S., Chow, L. M., Baker, S. J., Sorrentino, B. P., and Dyer, M. A. (2009) *Proc. Natl. Acad. Sci. U.S.A.* **106,** 6685–6690
26. Chen, C. M., and Cepko, C. L. (2000) *Mech. Dev.* **90,** 293–297
27. André, E., Gawlas, K., and Becker-André, M. (1998) *Gene* **216,** 277–283
28. Chen, S., Wang, Q. L., Nie, Z., Sun, H., Lennon, G., Copeland, N. G., Gilbert, D. J., Jenkins, N. A., and Zack, D. J. (1997) *Neuron* **19,** 1017–1030
29. Furukawa, T., Morrow, E. M., and Cepko, C. L. (1997) *Cell* **91,** 531–541
30. Nishida, A., Furukawa, A., Koike, C., Tano, Y., Aizawa, S., Matsuo, I., and Furukawa, T. (2003) *Nat. Neurosci.* **6,** 1255–1263
31. Chatelain, G., Fossat, N., Brun, G., and Lamonerie, T. (2006) *J. Mol. Med.* **84,** 604–615
32. Srinivas, M., Ng, L., Liu, H., Jia, L., and Forrest, D. (2006) *Mol. Endocrinol.* **20,** 1728–1741
33. Kautzmann, M. A., Kim, D. S., Felder-Schmittbuhl, M. P., and Swaroop, A. (2011) *J. Biol. Chem.* **286,** 28247–28255
34. Koike, C., Nishida, A., Ueno, S., Saito, H., Sanuki, R., Sato, S., Furukawa, A., Aizawa, S., Matsuo, I., Suzuki, N., Kondo, M., and Furukawa, T. (2007) *Mol. Cell Biol.* **27,** 8318–8329
35. Hyatt, G. A., Schmitt, E. A., Fadool, J. M., and Dowling, J. E. (1996) *Proc. Natl. Acad. Sci. U.S.A.* **93,** 13298–13303
36. Liu, H., Etter, P., Hayes, S., Jones, I., Nelson, B., Hartman, B., Forrest, D., and Reh, T. A. (2008) *J. Neurosci.* **28,** 749–756
37. Swain, P. K., Hicks, D., Mears, A. J., Apel, I. J., Smith, J. E., John, S. K., Hendrickson, A., Milam, A. H., and Swaroop, A. (2001) *J. Biol. Chem.* **276,**

36824–36830
38. Oh, E. C., Khan, N., Novelli, E., Khanna, H., Strettoi, E., and Swaroop, A. (2007) *Proc. Natl. Acad. Sci. U.S.A.* **104,** 1679–1684
39. Graf, T., and Enver, T. (2009) *Nature* **462,** 587–594
40. Alvarez-Delfin, K., Morris, A. C., Snelson, C. D., Gamse, J. T., Gupta, T., Marlow, F. L., Mullins, M. C., Burgess, H. A., Granato, M., and Fadool, J. M. (2009) *Proc. Natl. Acad. Sci. U.S.A.* **106,** 2023–2028
41. Rhead, B., Karolchik, D., Kuhn, R. M., Hinrichs, A. S., Zweig, A. S., Fujita, P. A., Diekhans, M., Smith, K. E., Rosenbloom, K. R., Raney, B. J., Pohl, A., Pheasant, M., Meyer, L. R., Learned, K., Hsu, F., Hillman-Jackson, J., Harte, R. A., Giardine, B., Dreszer, T. R., Clawson, H., Barber, G. P., Haussler, D., and Kent, W. J. (2010) *Nucleic Acids Res.* **38,** D613–619